



POTSDAM-INSTITUT FÜR
KLIMAFOLGENFORSCHUNG

Originally published as:

Piniewski, M., Mezghani, A., Szczesniak, M., Kundzewicz, Z. W. (2017): Regional projections of temperature and precipitation changes: Robustness and uncertainty aspects. - Meteorologische Zeitschrift, 26, 2, 223-234

DOI: [10.1127/metz/2017/0813](https://doi.org/10.1127/metz/2017/0813)

Regional projections of temperature and precipitation changes: Robustness and uncertainty aspects.

MIKOŁAJ PINIEWSKI^{1,2*}, ABDELKADER MEZGHANI³, MATEUSZ SZCZEŚNIAK¹ and ZBIGNIEW W. KUNDZEWICZ^{2,4}

¹Warsaw University of Life Sciences, Poland

²Potsdam Institute for Climate Impact Research, Germany

³Norwegian Meteorological Institute, Norway

⁴Institute of Agricultural and Forest Environment of the Polish Academy of Sciences, Poland

(Manuscript received October 17, 2016; in revised form December 11, 2016; accepted December 12, 2016)

Abstract

This study presents the analysis of bias-corrected projections of changes in temperature and precipitation in the Vistula and Odra basins, covering approximately 90 % of the Polish territory and small parts of neighbouring countries in Central and Eastern Europe. The ensemble of climate projections consists of nine regional climate model simulations from the EURO-CORDEX ensemble for two future periods 2021–2050 and 2071–2100, assuming two representative concentration pathways (RCPs) 4.5 and 8.5. The robustness is measured by the ensemble models' agreement on significant changes. We found a robust increase in the annual mean of daily minimum and maximum temperature, by 1–1.4 °C in the near future and by 1.9–3.8 °C in the far future (areal-means of the ensemble mean values). Higher increases are consistently associated with minimum temperature and the gradient of change goes from SW to NE regions. Seasonal projections of both temperature variables reflect lower robustness and suggest a higher future increase in winter temperatures than in other seasons, notably in the far future under RCP 8.5 (by more than 1 °C). However, changes in annual means of precipitation are uncertain and not robust in any of the analysed cases, even though the climate models agree well on the increase. This increase is intensified with rising global temperatures and varies from 5.5 % in the near future under RCP 4.5 to 15.2 % in the far future under RCP 8.5. Spatial variability is substantial, although quite variable between individual climate model simulations. Although seasonal means of precipitation are projected to considerably increase in all four combinations of RCPs and projection horizons for winter and spring, the high model spread reduces considerably the robustness, especially for the far future. In contrast, the ensemble members agree well that overall, the summer and autumn (with exception of the far future under RCP 8.5) precipitation will not undergo statistically significant changes.

Keywords: EURO-CORDEX, temperature projections, precipitation projections, robustness, model uncertainty, Poland

1 Introduction

1.1 Motivation

Increase of mean annual air temperature has been detected at various spatial scales, ranging from local to national, regional, continental, hemispheric, and global (KUNDZEWICZ and HUANG, 2010; STANISŁAWSKA *et al.*, 2013; IPCC, 2013). The increase of globally averaged combined land and ocean surface temperature, over the period 1880 to 2012, was about 0.85 [0.65 to 1.06] °C (IPCC, 2013). Each individual year since 2001 belongs to the 16 globally warmest years in the history of global instrumental observations, i.e. since 1880 (the only pre-2001 year in this list being 1998). FORTUNIAK *et al.* (2001) and KOZUCHOWSKI and ŻMUDZKA (2001) found a temperature increase of 0.8 °C for the area of Poland in the second half of the 20th century. LIMANÓWKA

et al. (2012) extended the analysis to cover the more recent interval 1951–2008. In 1951–2008, the trend in the spatially-averaged air temperature for the whole area of Poland was 0.24 °C per decade, whereas the fastest rise was observed on the coasts (0.27 °C/decade) and the lowest in the highlands (0.19 °C/decade). On the seasonal scale, the strongest increase of spatially-averaged observed seasonal air temperature occurred in winter and spring (0.38 °C/decade and 0.36 °C/decade, respectively), while the smallest and statistically insignificant increase occurred in autumn (0.06 °C/decade). In further years, after the year 2008, temperature has shown a higher increase, followed by years 2014 and 2015 beating all-time records at many stations in Poland. As far as changes in annual precipitation totals in Poland are concerned, significant changes were observed neither in the whole country nor in the sub regions. What was observed was a strong variation from year to year.

Few studies related to projections of climate change have been dedicated to Poland. For instance, climate projections originating from the ENSEMBLES project

*Corresponding author: Mikołaj Piniewski, Warsaw University of Life Sciences, Poland, e-mail: mpiniewski@levis.sgw.pl

(VAN DER LINDEN and MITCHELL, 2009) were the basis for investigations of extreme climatic indices relevant for different sectors (agriculture, water resources and health) (SZWED et al., 2010), winter thermal conditions (PIOTROWSKI and JĘDRUSZKIEWICZ, 2013), as well as those issued from the 'KLIMADA' project (<http://klimada.mos.gov.pl/en/>), within the framework of the Polish National Adaptation Strategy to Climate Change (NAS 2020). In the latter project, eight bias-corrected regional climate models (RCMs) under the Special Report on Emission Scenarios (SRES) (VAN DER LINDEN and MITCHELL, 2009) A1B scenario were applied to estimate changes in climate variables and specific climate indices in two future horizons, 2021–2050 and 2071–2100. The outcomes of the latter project showed significant upward trend in temperature, and subsequently, significant changes in temperature-based indices, while precipitation projections were uncertain, suggesting slight increases in the median of winter changes and slight decreases in summer. PIOTROWSKI and JĘDRUSZKIEWICZ (2013) assessed the spatial variability in winter temperature over Poland for the 2021–2050 period based on three RCMs under SRES A1B scenario. The highest temperature increase was predicted in the North and the East of Poland, which was attributed to an increase of frequency of cyclonic circulation types. The magnitude of changes largely differed between climate models. SZWED et al. (2010) pointed out mainly unfavourable changes in Polish climate e.g. increased frequency of extreme events, reduced crop yields, and increased summer water budget deficit derived from six uncorrected regional climate model simulations under SRES A2 scenario. JACZEWSKI et al. (2015) compared changes of selected thermal indices for the time period 2011–2030 relative to 1971–1990, based on bias-corrected projections from the RegCM (REGional Climate Model) under SRES B1, A1B and A2 scenarios and reported an increase in the number of summer and hot days and a decrease in the number of frost and ice days.

More recently, even fewer studies have been done for Poland using a newer generation of climate model simulations such as the fifth generation of the Coupled Model Intercomparison Project (CMIP5) or the European domain of the Coordinated Downscaling Experiment Initiative (EURO-CORDEX). PLUNTKE et al. (2016) applied the statistical downscaling model WETTREG2013 for temperature and precipitation projections from two GCMs, one under two newer generation Representative Concentration Pathways (RCP) 2.6 and 8.5 scenarios, and one under SRES A1B, for the south-western part of Poland and eastern Saxony. Their results showed an acceleration of changes by the end of 21st century leading to negative consequences for the climatic water balance, particularly under SRES A1B and RCP 8.5. ROMANOWICZ et al. (2015) corrected modelled temperature and precipitation of seven GCM-RCM combinations from EURO-CORDEX over ten Polish catchments. They pointed out that bias-corrected projections

under RCP 4.5 agreed quite well on a precipitation increase in the range 0–15 % depending on the catchment and future horizon, and an upward trend in temperature by 1 °C in 2021–2050, which is doubled by the end of the 21st century.

1.2 Mapping climate model robustness

Even though an ensemble approach is now recognised as a standard in climate change science, aggregation of projections from different ensemble members, often counted in tens, into a single, informative and stakeholder-friendly map has always posed various challenges. On the one hand, the uncertainty in successive generations of climate models remains large despite considerable progress in terms of simulating atmospheric and climatic processes in greater detail, hence, projections from different models often diverge with a rate depending on various factors such as geographic location, weather or climate variable, and season. On the other hand, producing exclusively maps of multi-model ensemble mean or median change, still common in regional-scale studies, remain insufficient. For instance, when analysing climate projections from multiple models for a given location, two properties can be assessed: agreement between models (ideally quantified by one value per ensemble) and statistical significance of change according to each model (n values for n ensemble members). A combination of these two properties is often referred to as robustness (KNUTTI and SEDLÁČEK, 2013; PFEIFER et al., 2015). While assessing statistical significance is rather straightforward, various approaches have been developed to measure the model agreement. The number of models agreeing on the sign of change has been adopted in the 4th Assessment Report of the Intergovernmental Panel of Climate Change (IPCC, 2007), in the first assessment report of the EURO-CORDEX projections (JACOB et al., 2014) and in other isolated studies (VAUTARD et al., 2014; PFEIFER et al., 2015). Various forms of uncertainty versus signal, or signal-to-noise ratio, exist such as the ratio of one standard deviation across the multi-model range over the multi-model mean change (FISCHER et al., 2014). Finally, KNUTTI and SEDLÁČEK (2013) adopted the robustness R measure based on the integrals of three cumulative density functions: one characterising all individual model projections (CDF1), the second one representing the multi-model mean projection (CDF2), and the third one representing the multi-model mean of the historical climate (CDF3). Comparison of CDF2 with CDF1 measures uncertainty, and comparison of CDF2 with CDF3 measures signal. This approach has some advantages over other existing methods, as it holistically considers the magnitude of change, the sign, natural variability and inter-model spread.

The robustness of climate projections R has been used in a number of studies as a measure of models' agreement in simulating the climate change signal, both at global (SEDLÁČEK and KNUTTI, 2014; PROESTOS et al., 2015) and regional (LIEVELD et al., 2016) scale.

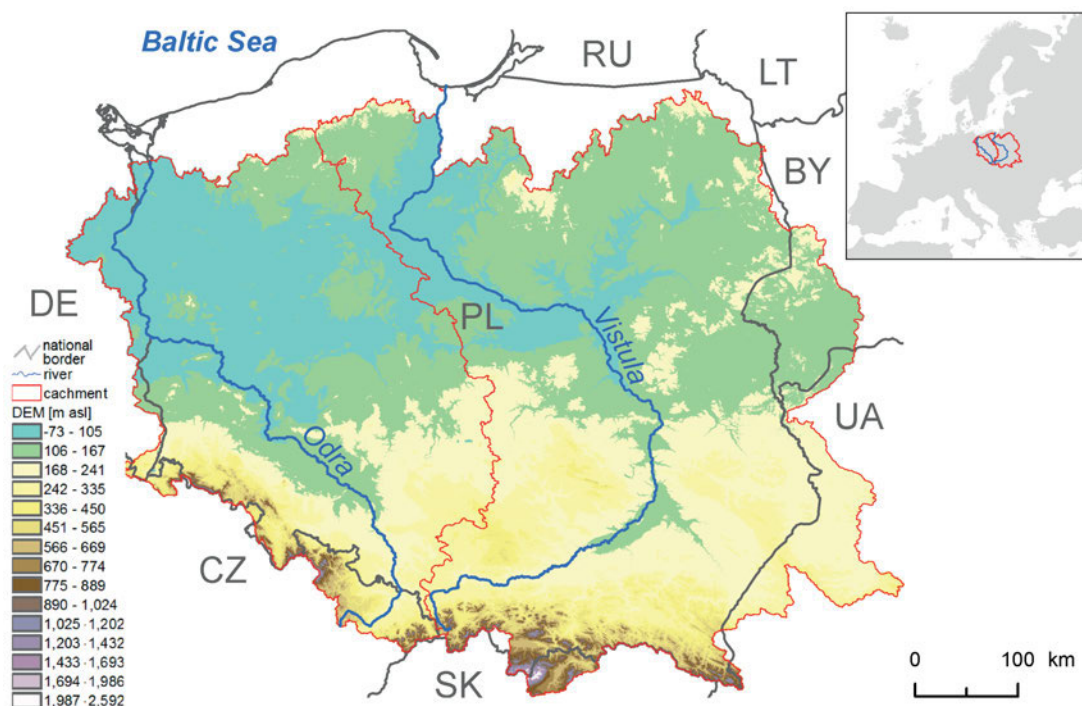


Figure 1: Study area showing Poland (PL, black lines) and Odra and Vistula catchments (red lines). Colours give height above sea level.

1.3 Objective

The main objective of this paper is to evaluate an ensemble of annual and seasonal projections of daily minimum and maximum temperature and total precipitation over the basins of two largest Polish rivers, the Vistula and the Odra. The climate projections used here were based on an ensemble of bias-corrected EURO-CORDEX simulations under two RCPs (4.5 and 8.5) for two future horizons within the 21st century. The secondary objective is to assess and provide robustness maps related to these projections over Poland, following the approach of [KNUTTI and SEDLÁČEK \(2013\)](#).

2 Materials and methods

2.1 Study area

The Vistula and Odra basins (VOB) have been selected for this study as they are the main focus region of climate impact modelling within the CHASE-PL project (Climate Change Impacts for Selected Sectors in Poland, <http://www.chase-pl.pl/>). They are located in Central and Eastern Europe, covering most of Poland and parts of neighbour countries (Germany, Czech Republic, Slovakia, Ukraine and Belarus), and draining their waters to the southern part of the Baltic Sea (Figure 1). They occupy 193,831 and 119,041 km², of which 87 % and 88 %, respectively, lie in Poland. The great majority of both drainage areas spans through the North European Plains, while the southern belt of both basins has a mountainous character. Poland has a temperate climate

with cold winters and warm summers, which is influenced by air masses from all directions: maritime from the west, cold polar air from Russia and Scandinavia, as well as sub-tropical air from the Atlantic Ocean, Mediterranean, and Black Sea.

2.2 Bias-corrected dataset of temperature and precipitation projections

Correcting the present climate to be closer to observations has been a mandatory step for most climate change impact studies ([SORTEBERG et al., 2014](#)). The CHASE-PL Climate Projections – Bias Corrected Daily Precipitation and Temperature 5 km (CPLCP-BCDPT5) dataset ([MEZGHANI et al., 2016](#)) was used here for studying projected climate change in the VOB. This dataset contains projections of daily values of three variables (minimum temperature T_{\min} , maximum temperature T_{\max} and precipitation P) from a multi-model ensemble (MME) of nine EURO-CORDEX GCM-run-RCM combinations for the historical period (1971–2000) and two future periods (2021–2050 – labelled as near future, and 2071–2100 – far future), each under two RCPs (4.5 and 8.5) (Table 1). Selected climate model simulations consisted of combinations of four GCMs and four RCMs and were bias-corrected using the quantile mapping method (R package ‘qmap’ developed by the Norwegian Meteorological Institute, [GUDMUNDSSON et al. \(2012\)](#)). This non-parametric method has shown a good performance compared to other bias correction methods in reproducing not only the mean but also the standard deviation and extremes ([THEMESSL et al., 2010](#)).

Table 1: List of available GCM-run-RCM combinations composing the multi-model ensemble (MME). Each combination was available for the historical period (1971–2000) and two future periods (2021–2050 and 2071–2100) under two RCPs (4.5 and 8.5).

Code	GCM	RCM
01	CNRM-CERFACS-CNRM-CM5	CLMcom-CCLM4-8-17
02	CNRM-CERFACS-CNRM-CM5	SMHI-RCA4
03	ICHEC-EC-EARTH	CLMcom-CCLM4-8-17
04	ICHEC-EC-EARTH	SMHI-RCA4
05	ICHEC-EC-EARTH	KNMI-RACMO22E
06	ICHEC-EC-EARTH	DMI-HIRHAM5
07	IPSL-IPSL-CM5A-MR	SMHI-RCA4
08	MPI-M-MPI-ESM-LR	CLMcom-CCLM4-8-17
09	MPI-M-MPI-ESM-LR	SMHI-RCA4

The CHASE-PL Forcing Data – Gridded Daily Precipitation & Temperature Dataset 5 km (CPLFD-GDPT5) (BEREZOWSKI et al., 2016) was used as reference in calibration procedure. Thus, quantiles of the simulations for the control period (1971–2000) were mapped onto corresponding quantiles in the observations (1951–2013, as the most recent 63-years reference time period) and the bias in the daily temperature and precipitation simulations was removed. In order to take into account the seasonality in the observations, bias correction was applied on each of the four seasons separately. Furthermore, the bias-corrected set-up included a linear interpolation between the fitted and simulated values lying outside the range of observed data in the training period. The same correction found for the highest percentile to extrapolate for values falling outside the range of the observed climate was applied, as in Boé et al. (2007). Furthermore, the method included an adjustment of wet-day frequencies for precipitation and was applied to the four seasons separately.

In the present study, all data were re-interpolated from the original 5 km resolution of the CPLCP-BCDPT5 dataset on the layer of 2633 sub-basins from the SWAT model of the VOB developed in PINIEWSKI et al. (in review), with a purpose of running climate change scenarios. Sub-basin sizes were variable, with mean area equal to 111 km². Three first years of both historical and future periods were truncated, since a warm-up period of three years is used for SWAT simulations. The climate change for the two future horizons with regards to the reference period was expressed in terms of relative changes for annual and seasonal sums of P (in %) and in terms of absolute changes for annual and seasonal means of daily T_{\min} and T_{\max} (in °C). This procedure was applied for each climate model, future horizon, RCP and temporal aggregation (annual or one of four seasons), thus leading to $9 \times 2 \times 2 \times 5 = 180$ maps for each of the three analysed variables. While maps for different periods and different RCPs should be kept separately, it was desired to significantly reduce the number of maps for different climate model simulations, aggregating them in a scientifically-defensible manner.

2.3 Robustness estimation

A robustness measure R similar to that proposed by KNUTTI and SEDLÁČEK (2013) is used here as a measure of models' agreement and is calculated locally for each sub region and spatial entity. It should be noted that this quantitative measure combines two essential properties when dealing with ensemble of climate projections: the signal-to-noise ratio and a skill score. While the technical details of its calculation are available in the paper of KNUTTI and SEDLÁČEK (2013), here we present some key features:

- R values are influenced by models' spread and magnitude of the signal.
- It considers the width of the initial distributions (such that the same projection has a lower R value if the variability is small).
- It penalizes (by covering the ensemble mean map with a white colour) the case when models agree on the sign and significance but considerably disagree on the magnitude.
- The value of R increases with lower model spread or higher magnitude of signal. The maximum value is 1 and the values below 0 are considered very low. KNUTTI and SEDLÁČEK (2013) used a threshold of 0.8 over which “models agree on significant change”.

The robustness categories are determined based on the value of R and the fraction of models with statistically significant change (denoted as ν_s) at $p = 0.05$ level, using the Mann-Whitney U test. The robustness maps are constructed so that i) the colours show the multi-model mean change, ii) stippling represents R values higher than 0.6 (good agreement), iii) hatching marks areas where $\nu_s \leq \frac{1}{9}$ (agreement on no change), and iv) white colour indicates areas where $\nu_s \geq \frac{6}{9}$ and $R \leq 0.3$, i.e. significant changes but little agreement among models. Moreover, the areas where no graphical pattern is super-imposed on the map, could be seen as regions with limited evidence for change in the indicated direction. In line with suggestions of KNUTTI and SEDLÁČEK (2013), we adapted the threshold values for R (decreased by 0.2) compared to their work. The graphical illustration of the above criteria can be found in the Supplementary Material Figure S1.

3 Results

3.1 Temperature projections

Figures 2 and 3 show changes in annual mean of daily minimum and maximum temperature for the near and far future, under RCPs 4.5 and 8.5, respectively. Climate warming is ubiquitous and robust (represented by the stippling marks across the whole domain), with an exception made for T_{\max} projections in the near future under RCP 4.5 for which R was slightly below 0.6 in the majority of the study area. The figures show a

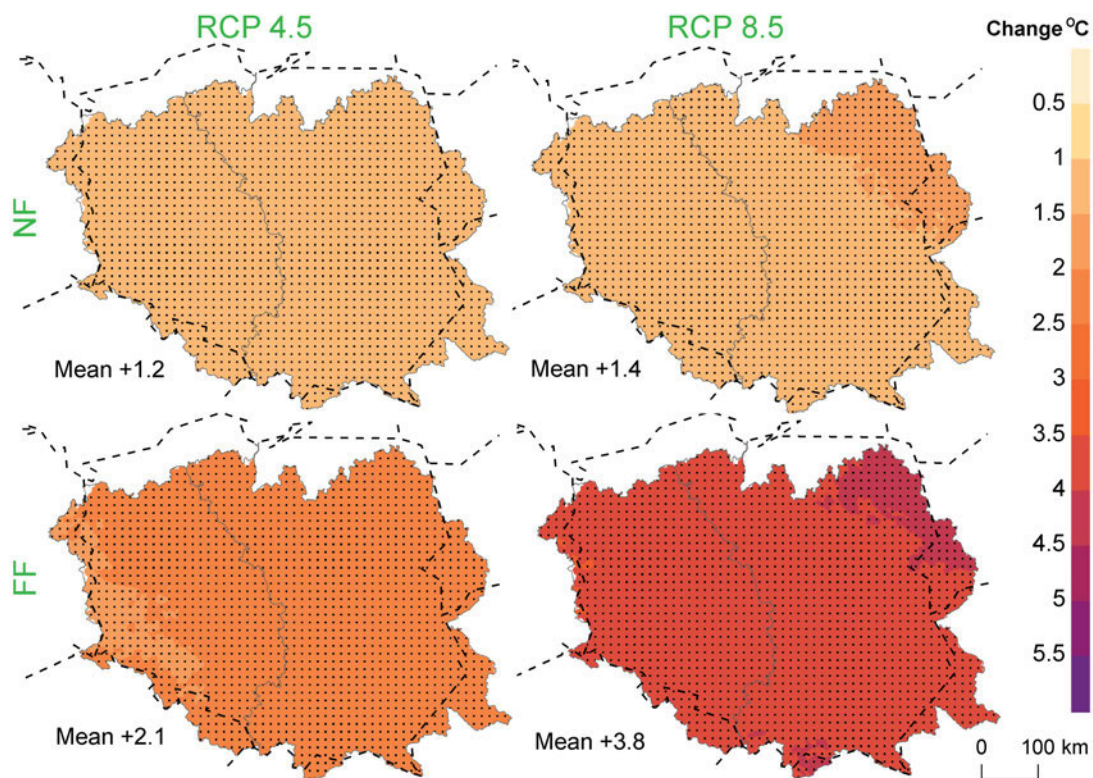


Figure 2: Multi-model ensemble mean change in annual means of daily minimum temperature for the near and far future under RCPs 4.5 and 8.5. Values in the left bottom corner of each map mark mean areal changes for a given map. Black, dashed line marks Poland and neighbouring countries contours, whereas grey, solid line divides the basins of the Vistula (right) and the Odra (left) rivers. *Stippling* marks areas with high model agreement, *hatching* marks areas where less than 20% of models show a significant change, *white* marks areas with inconsistent model response, whereas *colours without stippling and hatching* can be interpreted as regions with limited evidence for change in the indicated direction (after (KNUTTI and SEDLÁČEK, 2013)).

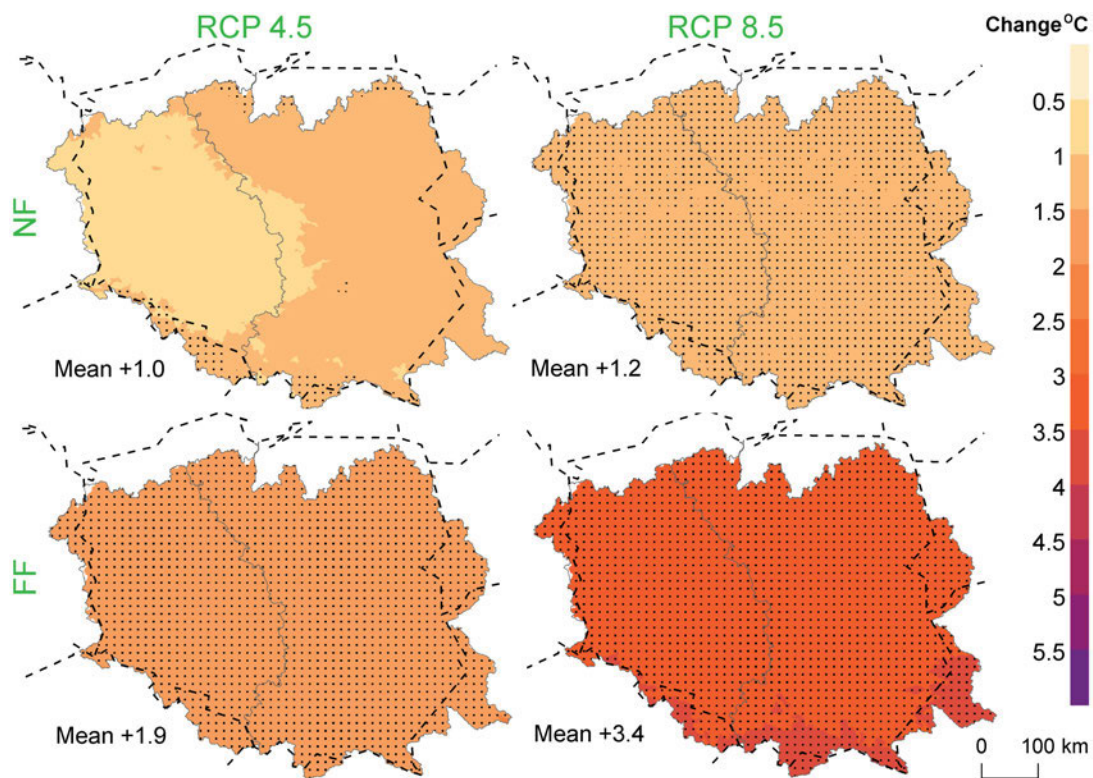


Figure 3: Multi-model ensemble mean change in annual means of daily maximum temperature for the near and far future under RCPs 4.5 and 8.5. The remaining symbols as in Figure 2.

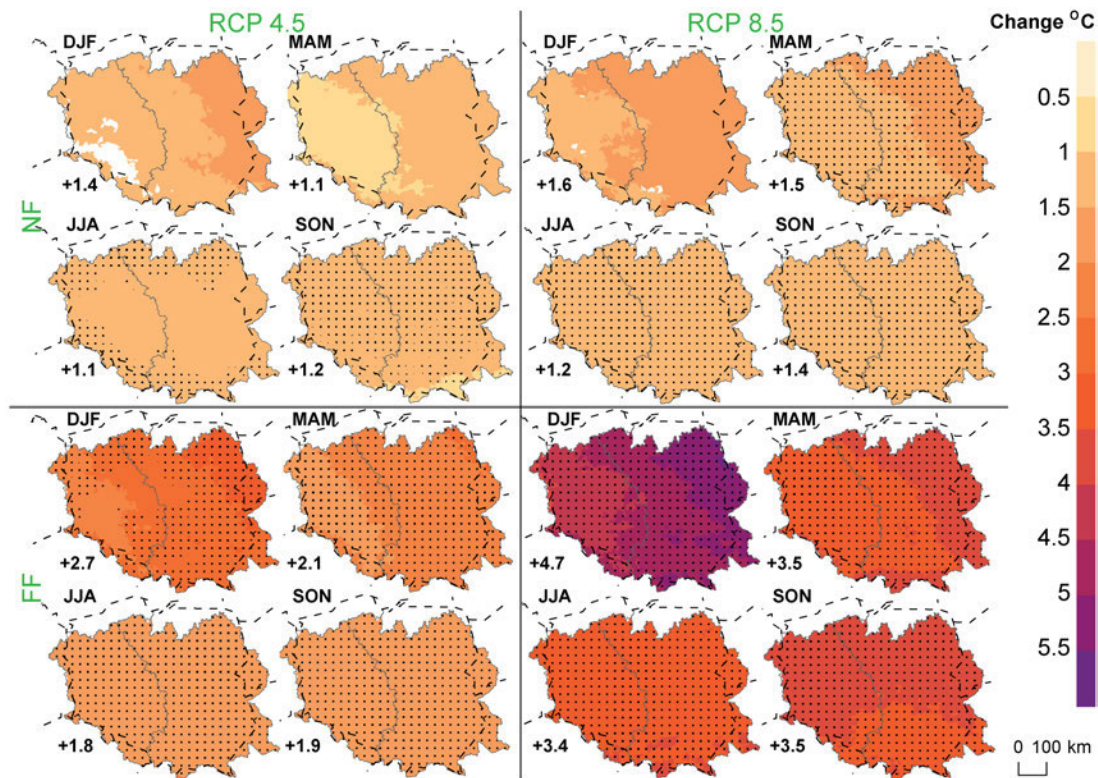


Figure 4: Multi-model ensemble mean change in seasonal means of daily minimum temperature for the near and far future under RCPs 4.5 and 8.5. The remaining symbols as in Figure 2. DJF, MAM, JJA and SON stand for standard climatological abbreviations for winter, spring, summer and autumn, respectively.

small difference (by 0.2°C) between RCPs in the near future which becomes much larger in the far future (by $1.5\text{--}1.7^{\circ}\text{C}$). The acceleration of warming with time is more rapid under the RCP 8.5 than RCP 4.5 for both variables. In all cases (for all time horizons and RCPs), the projected increase in T_{max} is by far lower than the corresponding increase in T_{min} , although the difference is small (less than 0.4°C). This leads to a decrease in projected daily temperature amplitude.

For daily temperature, the spatial variability in projected change is generally low. The difference between the highest and lowest projected change within one map does not exceed 0.7°C , with one exception (T_{min} in the far future under RCP 8.5) and the standard deviation calculated across all sub-basins is always lower than 0.15°C . Thus, spatial gradients are not easy to detect. For minimum temperature, there is a SW-NE gradient, relatively consistent across time periods and RCPs. Contrary, the spatial gradient goes from west to east for maximum temperature for RCP 4.5 in both time horizons, and shows an inconsistent pattern between the two periods under RCP 8.5. This may be due to the fact that our analysis is based on the MME mean, which does not have any physical interpretation in contrast to a single climate model simulation.

Figures 4 and 5 illustrate seasonal projections of T_{min} and T_{max} , and the assessment of their robustness. It can be seen that in all cases (both near and far future time periods and under both RCPs) winter temperature increase

is the highest. Yet, this difference is much higher in the far future than in the near future. Robustness of seasonal projections is much lower than of the annual ones (Figure 6) which is mainly due to less variability on that temporal scale. Spatial trends are weak and sometimes non-existent, such as for the mean annual temperature. For T_{max} projections are robust only in the far future under RCP 8.5, whereas for T_{min} they are robust for the far future under both RCPs. In contrast, in the near future there are areas, particularly large for summer T_{max} , for which the climate model response seems to be inconsistent, despite the fact that the MME mean increase is $0.9\text{--}1.0^{\circ}\text{C}$ and all models agree on the sign of the change.

Although spatial variability in seasonal minimum and maximum temperature is generally low, as compared with annual maps, there is a clear SW-NE gradient for spring T_{min} (less clear, but also present for spring T_{max}) and an W-E gradient for winter T_{min} (slightly more variable for winter T_{max}), consistent across future time horizons and RCPs. For example, an increase in winter T_{min} in the far future under RCP 8.5 is projected to be lower than 4°C for the western part of the Odra basin and to be higher than 5.5°C in the eastern part of the Vistula basin. A less consistent trend is observed for autumn T_{min} , whose increase is the highest in the north (or north-east) and the lowest in the south (or south-east). Spatial trends for summer T_{min} depend on the RCP and time period. While spatial patterns in

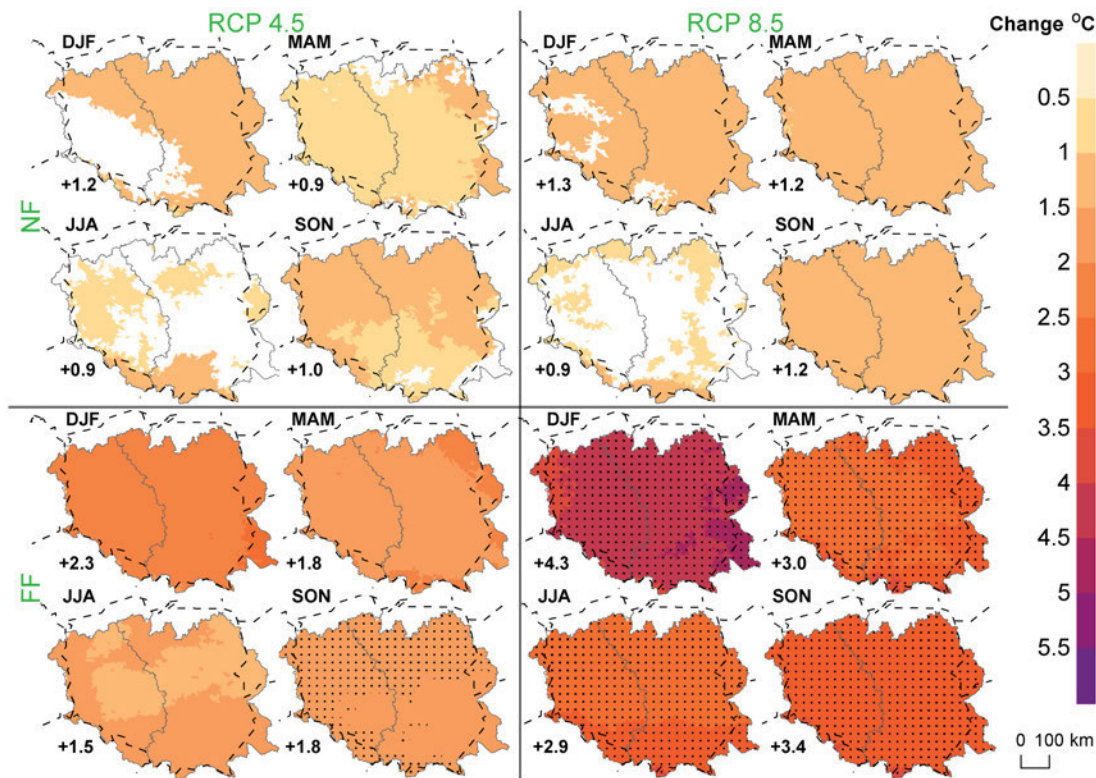


Figure 5: Multi-model ensemble mean change in seasonal means of daily maximum temperature for the near and far future under RCPs 4.5 and 8.5. The remaining symbols as in Figure 2.

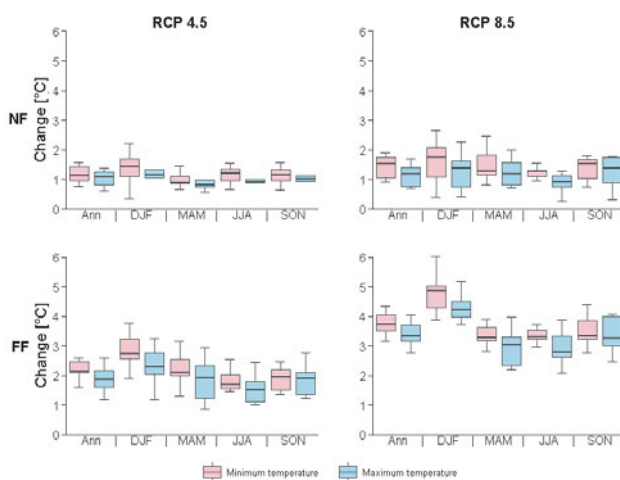


Figure 6: Box plots of projected changes in minimum and maximum temperature calculated across different climate models for annual (ANN) and seasonal precipitation in the near (NF) and far (FF) future under RCP 4.5 and 8.5.

autumn T_{max} are largely inconsistent, those for summer T_{max} are consistent between two RCPs in the far future (NE-SW). For the near future they are not analysed, as the climate models do not provide sufficiently robust result.

3.2 Precipitation projections

Annual total precipitation is projected to increase throughout almost the entire VOB (Figure 7), and ac-

ording to all climate models (Figure 8), with rates dependent on the RCP and time horizon, ranging between 5.5 % and 15.2 % (spatial average). The increase accelerates with time and emissions. None of the projected changes are robust, and in some sub-areas, notably north-east for the RCP 4.5 in the far future, and south-east for the RCP 8.5 in the far future, the model response is inconsistent. There are also areas, where the models agree on the lack of significance (hatching areas), in particular in the near future under RCP 4.5 in the southern parts of the basins.

The magnitude of precipitation increase is the lowest in the south east of the VOB in the near future and in the south in the far future. Spatial differences between the highest and lowest change are substantial for the far future under RCP 8.5 (an increase by more than 20 % in some isolated areas in the NE corner compared to an increase by less than 5 % in some areas in the south), and moderate (below 10 %) for the remaining cases. As shown in the Supplementary Material Figure S2 (projections for the far future under RCP 4.5), individual climate model simulations tend to exhibit rather different spatial patterns.

A more clear pattern is visible for seasonal precipitation projection (Figure 9), showing an areal-mean increase for all seasons and all horizon-RCP combinations. However, the rate of the change is more intensified in winter and spring than in summer and autumn. While the increase in winter and spring precipitation is ubiquitous, changes in summer and autumn precipitation have different signs depending on location, RCP

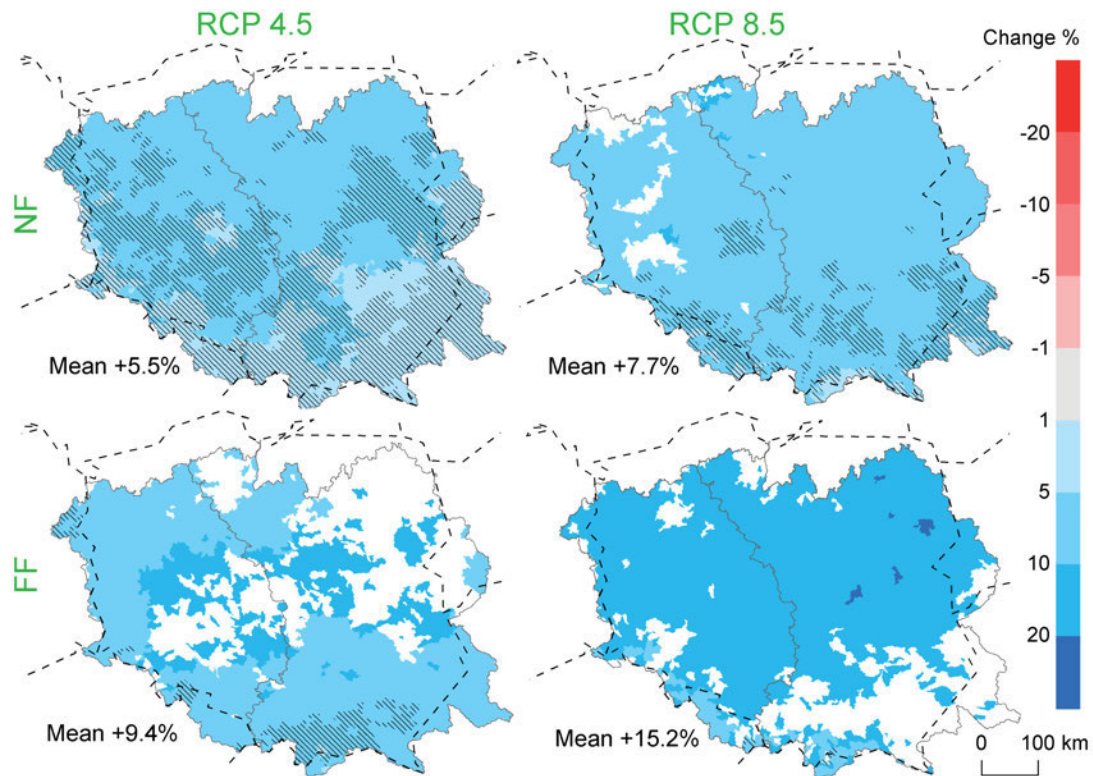


Figure 7: Multi-model ensemble mean change in annual total precipitation for the near and far future under RCPs 4.5 and 8.5. The remaining symbols as in Figure 2.

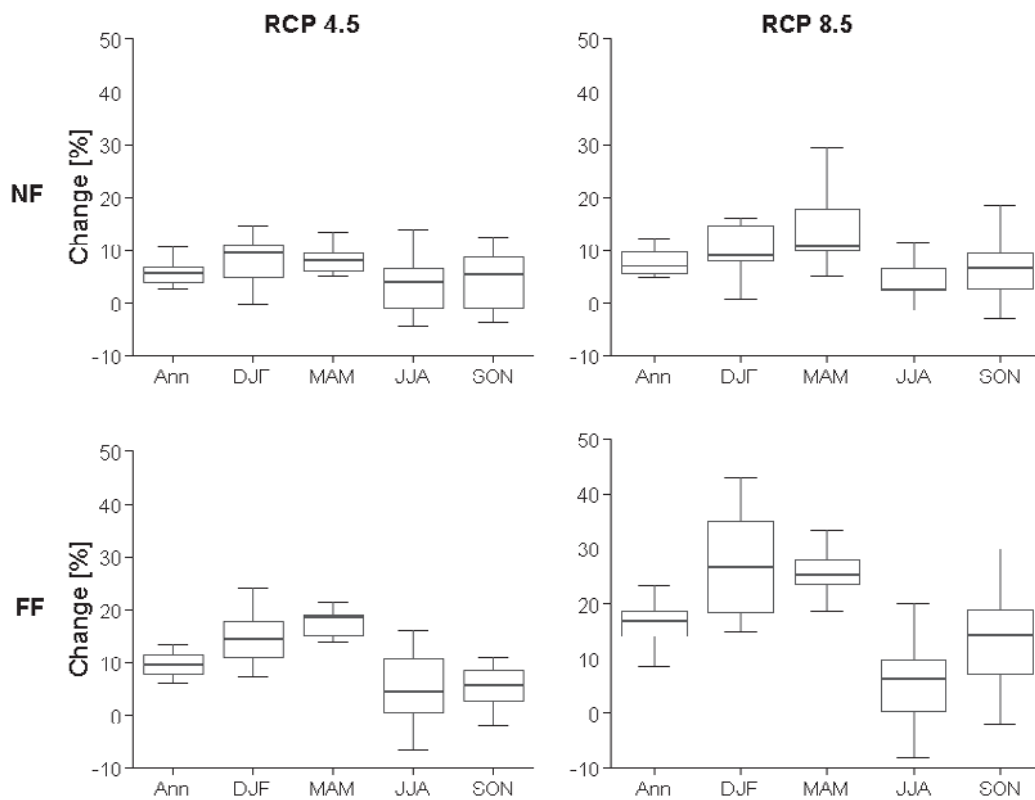


Figure 8: Box plots of projected changes in total precipitation calculated across different climate models for annual (ANN) and seasonal precipitation in the near (NF) and far (FF) future under RCP 4.5 and 8.5.

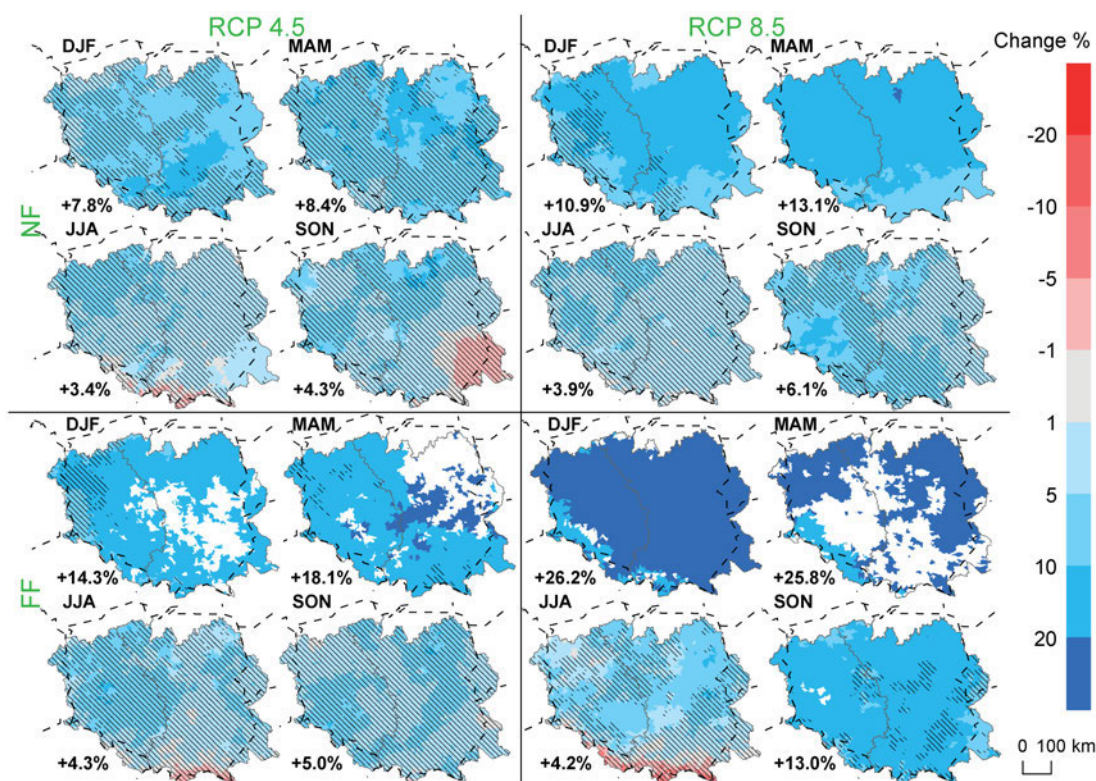


Figure 9: Multi-model ensemble mean change in seasonal total precipitation for the near and far future under RCPs 4.5 and 8.5. The remaining symbols as in Figure 2.

and time horizon. Yet, the magnitude of these changes, either positive or negative, is usually lower compared to internal climate variability, hence, there is an agreement on no significant change (with exception of autumn precipitation in the far future under RCP 8.5). Interestingly, white areas in the maps indicate model disagreement which is super-imposed over large parts of the VOB with cases showing the highest overall magnitude of increase (25.8% for spring precipitation in the far future under RCP 8.5). Even though all ensemble members agree on the increase and its mean is very high, the uncertainty related to its magnitude is higher than the signal.

Spatial variability of changes in seasonal precipitation is substantial but the patterns are more complex than for temperature maps, with less clear gradients. Autumn precipitation is projected to decrease (or its increase is the lowest) in the eastern part of the Vistula basin for each RCP and time period. However, these results should be treated with caution, as most of them were assessed as the lack of significant change.

4 Discussion

The EURO-CORDEX simulations constitute the current state-of-the-art of climate projections over Europe (JACOB et al., 2014). In particular, a sub-set of projections available at the highest resolution of 0.11° has been shown to have the added value over the coarser-scale, 0.44° projections in the case of precipitation on

local scales, up to 400 km (PREIN et al., 2016). Still, the EURO-CORDEX projections have considerable biases and there is only limited evidence for an added value of the higher resolution in the precipitation intensity and frequency (CASANUEVA et al., 2016). Correcting the bias in climate projections is of vital importance for impact modelling, which is why the CHASE-PL project has put a considerable emphasis on deriving a high-resolution gridded product serving as the reference for bias correction of the EURO-CORDEX simulations over Poland (BEREZOWSKI et al., 2016; MEZGHANI et al., 2016).

Our study shows that while there remains a considerable uncertainty in future climate projections among the EURO-CORDEX ensemble members (of which nine were used here), there are cases where robust signals can be found. We showed that projections of the annual mean of minimum temperatures (T_{\min}) are robust for both future periods under both RCPs over the entire domain. Similar changes for T_{\max} are not robust only for the RCP 4.5 in the near future, for which the magnitude of increase is the lowest (1°C). The robustness is lower for seasonal temperature projections: only for RCP 8.5 in the far future changes in both T_{\min} and T_{\max} are fully robust. For T_{\min} it is also the case for most of the area under RCP 4.5 in the far future and under RCP 8.5 in the near future. In contrast, for T_{\max} there are several cases for which an inconsistent model response was assessed for the majority of the VOB in the near future under both RCPs, in particular for summer temperature.

Perhaps the only study that also quantified robustness of the (uncorrected) EURO-CORDEX simulations for the domain covering the VOB is the one of JACOB et al. (2014). They applied a different method, adapted from PFEIFER et al. (2015), that uses the percentage of models agreeing on the direction of change and the statistical significance of changes from different models as the principal measures quantifying robustness. In agreement with our study, they showed that changes in mean annual temperature are significant and robust for the far future under both RCPs. The magnitude of the ensemble mean changes in their study was comparable to our estimates (from the ensemble mean), which shows that the bias correction did not alter the signal of change. This is in accordance with the recent study of DOSIO (2016), who reported negligible differences between the bias-corrected and raw changes in mean winter and summer T_{\min} and T_{\max} under RCP 8.5 in the far future for the Eastern Europe region that geographically covered the VOB. Importantly, in some other regions, such as e.g. Scandinavia or Iberian Peninsula, this conclusion did not hold.

We also showed that projected precipitation changes are not robust, regardless of RCP, future horizon and temporal aggregation. However, we identified regions for which results for various conditions agree that projected changes are not significant (e.g. southern half of the VOB in the near future under RCP 4.5 for annual total P) or seasons for which changes are not significant for almost the entire area under all RCPs in all periods (summer). In contrast to temperature projections, for which the robustness was positively correlated with the magnitude of change, in the case of precipitation we can observe inconsistent model response (white areas, cf. Figure 9) for cases with the highest projected magnitude of increase (e.g. spring or winter P in the far future). This is a fundamental difference from the approaches quantifying robustness based on the number of models agreeing on a certain direction of change. Since in this case all nine models agreed on the increase in spring precipitation, such an approach would result in robust changes. Indeed, JACOB et al. (2014) assessed projected changes in annual total precipitation as significant and robust over the entire area of the VOB, under both RCPs in the far future, which does not corroborate our findings. In contrast, the approach of KNUTTI and SEDLÁČEK (2013) that we used here penalizes the fact that the model spread, quantified on the basis of future period CDFs, is higher than the signal (i.e. there is a low signal-to-noise ratio), even if the signal is strong and statistically significant. This shows that this method is more strict in quantifying robustness than the more simple approach that involves counting the models agreeing on the direction of changes. As regards the magnitude of change, the ensemble mean maps of JACOB et al. (2014) look fairly consistent with our ensemble mean maps, indicating an increase in annual P by 5–15 % over the VOB in RCP 4.5 (in our study the VOB-mean increase by 9.4 %) and a higher increase (two classes 5–15 % and

15–25 %, with a SW-NE gradient) for RCP 8.5 (in our study the VOB-mean increase by 15.2 %, and the same gradient). As with temperature, it shows that the signal of change is not considerably distorted by the bias correction. Again, this is consistent with the findings of DOSIO (2016) for winter and summer precipitation in Eastern Europe under RCP 8.5 in the far future.

It should be noted though, that robustness *sensu* KNUTTI and SEDLÁČEK (2013) is not a binary variable: it spans through the continuum of possibilities, determined by the values of R and the fraction of models showing statistically significant change ν_s . As an example, Figures S3 and S4 of the Supplementary Material show the spatial variability of R and ν_s for annual precipitation projections, illustrating the complexity behind the maps shown in Figure 7. For the sake of visual (map) presentations of projected climate variables, thresholds need to be chosen to delimit regions with robust signals (stippling), agreement on no change (hatching) and the lack of agreement (white colour). The thresholds that were used in this study include: two critical values of R , two thresholds for the fraction of models showing statistically significant changes, and the significance level of the test (Supplementary Material Figure S1). The choice of thresholds is somewhat subjective and clearly affects the results, e.g. spatial coverage of particular robustness categories, as discussed in more detail in PFEIFER et al. (2015).

5 Conclusions

We analysed the robustness of the climate change signal as simulated by an ensemble of nine bias-corrected regional climate models over the Vistula and Odra basins. It was assessed following KNUTTI and SEDLÁČEK (2013), with modified threshold values delimiting regions showing different robustness categories. The agreement is based on magnitude, the sign, and the significance of the change. We found a robust increase in the annual mean of minimum and maximum temperature over the whole investigated area and for each combination of future horizon with RCP. Further, the magnitude of the areal-mean change is similar for both RCPs in the near future (the MME mean of 1.2–1.4 °C for T_{\min} and 1.0–1.2 °C for T_{\max}), but the signal strongly diverges for the far future (2.1–3.8 °C for T_{\min} and 1.9–3.4 °C for T_{\max}). Furthermore, the signal is spatially uniform, although a weak SW-NE gradient can be observed in the ensemble mean maps. However, the seasonal means of T_{\min} and T_{\max} projections are generally less robust (or even inconsistent, as for summer T_{\max}) than their annual counterparts in the near future. They are robust, for all seasons, in the far future for T_{\min} under both RCPs, and for T_{\max} under RCP 8.5. The increase is distinctly higher for winter than for any other season according to the MME mean, notably for the far future under RCP 8.5, when it exceeds 1.3 °C for both T_{\min} and T_{\max} .

Although the investigated climate models agree on the sign of precipitation change, our analysis suggests

that annual total precipitation projections are not robust in any of the considered cases. In contrast, there are regions with an agreement on lack of significant change (near future under RCP 4.5) or inconsistent responses (far future). Projected areal-mean increase accelerates with rising temperatures (i.e. both in time and from RCP 4.5 to 8.5), from 5.5 % in the near future under RCP 4.5 to 15.2 % in the far future under RCP 8.5. Individual climate model simulations exhibit different spatial patterns, whereas the MME mean maps suggest that the magnitude of projected increase is the lowest in the south east of the VOB in the near future and in the south in the far future. In addition, precipitation change is not seasonally uniform, regardless of the time horizon and RCP. The increase in winter and spring is of comparable magnitude and accelerates with time and rising temperature, as annual P . However, in some regions in the far future (notably, spring under RCP 8.5) the model spread is much higher than the strong signal, and in consequence, winter and spring P projections are assessed as inconsistent.

Areal means of projected changes in summer and autumn P are in the range 0–10 % (apart from autumn in the far future under RCP 8.5 when the mean increase is 13 %), thus being much smaller than corresponding changes in winter and spring. In fact, for the majority of the studied domain these changes are assessed as “the agreement on no change”. The ability to distinguish between robustness, inconsistency and no change in a spatially-explicit, transparent and user-friendly manner is an added value compared to all previous studies on ensemble-based projections of climate change in Poland. This method could be used in future studies on projections of climatic extremes as well as on sector-specific projections derived using climate impact models (e.g. hydrological, vegetation and agricultural models).

Acknowledgments

Support of the project CHASE-PL (Climate change impact assessment for selected sectors in Poland) of the Polish–Norwegian Research Programme operated by the National Centre for Research and Development (NCBiR) under the Norwegian Financial Mechanism 2009–2014 in the frame of Project Contract No. Pol Nor/200799/90/2014 is gratefully acknowledged. The first author is grateful for support to the Alexander von Humboldt Foundation and to the Ministry of Science and Higher Education of the Republic of Poland. The underlying climate projections dataset can be obtained from the 4TU Research Data Centre at <https://data.4tu.nl/repository/uuid:e940ec1a-71a0-449e-bbe3-29217f2ba31d>. Ensemble statistics of all projections can also be browsed in the interactive Climate Impact geportal at <http://climateimpact.sggw.pl/map/proj/>.

References

- BEREZOWSKI, T., M. SZCZEŚNIAK, I. KARDEL, R. MICHAŁOWSKI, T. OKRUSZKO, A. MEZGHANI, M. PINIEWSKI, 2016: CPLFD-GDPT5: High-resolution gridded daily precipitation and temperature data set for two largest Polish river basins. – *Earth Sys. Sci. Data* **8**, 127–139. DOI: [10.5194/essd-8-127-2016](https://doi.org/10.5194/essd-8-127-2016).
- BOÉ, J., L. TERRAY, F. HABETS, E. MARTIN, 2007: Statistical and dynamical downscaling of the Seine basin climate for hydro-meteorological studies. – *Int. J. Climatol.* **27**, 1643–1655. DOI: [10.1002/joc.1602](https://doi.org/10.1002/joc.1602).
- CASANUEVA, A., S. KOTLARSKI, S. HERRERA, J. FERNÁNDEZ, J.M. GUTIÉRREZ, F. BOBERG, A. COLETTE, O.B. CHRISTENSEN, K. GOERGEN, D. JACOB, K. KEULER, G. NIKULIN, C. TEICHMANN, R. VAUTARD, 2016: Daily precipitation statistics in a EURO-CORDEX RCM ensemble: added value of raw and bias-corrected high-resolution simulations. – *Climate Dyn.* **47**, 719. DOI: [10.1007/s00382-015-2865-x](https://doi.org/10.1007/s00382-015-2865-x).
- DOSIO, A., 2016: Projections of climate change indices of temperature and precipitation from an ensemble of bias-adjusted high-resolution EURO-CORDEX. – *J. Geophys. Res. Atmos.* **121**, 5488–5511. DOI: [10.1002/2015JD024411](https://doi.org/10.1002/2015JD024411).
- FISCHER, E.M., J. SEDLÁČEK, E. HAWKINS, R. KNUTTI, 2014: Models agree on forced response pattern of precipitation and temperature extremes. – *Geophys. Res. Lett.* **41**, 8554–8562. DOI: [10.1002/2014GL062018](https://doi.org/10.1002/2014GL062018).
- FORTUNIAK, K., K. KOŻUCHOWSKI, E. ŻMUDZKA, 2001: Trendy i okresowość zmian temperatury powietrza w Polsce w drugiej połowie XX wieku. – *Przeł. Geofiz. XLVI* **4**, 283–303.
- GUDMUNDSSON, L., J.B. BREMNES, J.E. HAUGEN, T. ENGEN-SKAUGEN, 2012: Technical Note: Downscaling RCM precipitation to the station scale using statistical transformations—a comparison of methods. – *Hydrol. Earth Sys. Sci.* **16**, 3383–3390. DOI: [10.5194/hess-16-3383-2012](https://doi.org/10.5194/hess-16-3383-2012).
- IPCC (INTERGOVERNMENTAL PANEL ON CLIMATE CHANGE), 2007: Climate Change 2007: The Physical Science Basis. – Contribution of Working Group I to the Fourth Assessment Report of the Intergovernmental Panel on Climate Change. SOLOMON, S., D. QIN, M. MANNING, Z. CHEN, M. MARQUIS, K.B. AVERYT, M. TIGNOR, H.L. MILLER (Eds.). – Cambridge University Press, Cambridge, United Kingdom and New York, NY, USA.
- IPCC (INTERGOVERNMENTAL PANEL ON CLIMATE CHANGE), 2013: Summary for Policymakers. In: Climate Change 2013: The Physical Science Basis. Contribution of Working Group I to the Fifth Assessment Report of the Intergovernmental Panel on Climate Change STOCKER T.F., D. QIN, G-K. PLATTNER, M. TIGNOR, S.K. ALLEN, J. BOSCHUNG, A. NAUELS, Y. XIA, V. BEX, P.M. MIDGLEY (Eds.). – Cambridge University Press, Cambridge, United Kingdom and New York, NY, USA.
- JACOB, D., J. PETERSEN, B. EGGERT, A. ALIAS, O.B. CHRISTENSEN, L.M. BOUWER, A. BRAUN, A. COLETTE, M. DÉQUÉ, G. GEORGIEVSKI, E. GEORGOPOULOU, A. GOBIET, L. MENUT, G. NIKULIN, A. HAENSLER, N. HEMPELMANN, C. JONES, K. KEULER, S. KOVATS, N. KRÖNER, S. KOTLARSKI, A. KRIEGSMANN, E. MARTIN, E. VAN MEIJGAARD, CH. MOSELEY, S. PFEIFER, S. PREUSCHMANN, CH. RADERMACHER, K. RADTKE, D. RECHID, M. ROUNSEVELL, P. SAMUELSSON, S. SOMOT, J.F. SOUSSANA, C. TEICHMANN, R. VALENTINI, R. VAUTARD, B. WEBER, P. YIOU, 2014: EURO-CORDEX: new high-resolution climate change projections for European impact research. – *Reg. Env. Change* **14**, 563–578. DOI: [10.1007/s10113-013-0499-2](https://doi.org/10.1007/s10113-013-0499-2).
- JACZEWSKI, A., B. BRZOSKA, J. WIBIG, A. ALIAS, O.B. CHRISTENSEN, L.M. BOUWER, 2015: Comparison of temperature indices for three IPCC SRES scenarios based on RegCM sim-

- ulations for Poland in 2011–2030 period. – *Meteorol. Z.* **24**, 99–106. DOI: [10.1127/metz/2014/0457](https://doi.org/10.1127/metz/2014/0457).
- KNUTTI, R., J. SEDLÁČEK, 2013: Robustness and uncertainties in the new CMIP5 climate model projections. – *Nature Climate Change* **3**, 369–373. DOI: [10.1038/NCLIMATE1716](https://doi.org/10.1038/NCLIMATE1716).
- KOZUCHOWSKI, K., E. ŻMUDZKA, 2001: Ocieplenie w Polsce, skala i rozkład sezonowy zmian temperatury powietrza w drugiej połowie XX wieku. – *Przeł. Geofiz* **1-2**, 81–90.
- KUNDZEWICZ, Z.W., S. HUANG, 2010: Seasonal temperature extremes in Potsdam. – *Acta Geophys* **58**, 1115. DOI: [10.2478/s11600-010-0026-5](https://doi.org/10.2478/s11600-010-0026-5).
- LELIEVELD, J., Y. PROESTOS, P. HADJINICOLAOU, M. TANARTHE, E. TYRLIS, G. ZITTIS, 2016: Strongly increasing heat extremes in the Middle East and North Africa (MENA) in the 21st century. – *Climatic Change* **137**, 1–16. DOI: [10.1007/s10584-016-1665-6](https://doi.org/10.1007/s10584-016-1665-6).
- LIMANÓWKA, D., D. BIERNACIK, B. CZARNECKI, R. FARAT, J. FILIPIAK, T. KASPROWICZ, R. PYRC, G. URBAN, R. WÓJCIK, 2012: Zmiany i zmienność klimatu od połowy XX w. (Changes and variability of climate since mid 20th century). In: J. WIBIG and E. JAKUSIK (Eds) *Warunki klimatyczne i oceanograficzne w Polsce i na Bałtyku Południowym. Spodziewane zmiany i wytyczne do opracowania strategii adaptacyjnych w gospodarce krajowej. Część I. Zmiany klimatu, ich wpływ na środowisko naturalne Polski oraz określenie ich skutków ekonomicznych.* – Monografie IMGW-PIB, IMGW-PIB, Warsaw, Poland, 7–33.
- MEZGHANI, A., A. DOBLER, J.E. HAUGEN, 2016: CHASE-PL Climate Projections: 5-km Gridded Daily Precipitation & Temperature Dataset (CPLCP-GDPT5). – Norwegian Meteor. Inst. Dataset., DOI: [10.4121/uuid:e940ec1a-71a0-449e-bbe3-29217f2ba31d](https://doi.org/10.4121/uuid:e940ec1a-71a0-449e-bbe3-29217f2ba31d).
- PFEIFER, S., K. BÜLOW, A. GOBIET, A. HÄNSLER, M. MUDELSEE, J. OTTO, D. RECHID, C. TEICHMANN, D. JACOB, 2015: Robustness of Ensemble Climate Projections Analyzed with Climate Signal Maps: Seasonal and Extreme Precipitation for Germany. – *Atmosphere* **6**, 677–698. DOI: [10.3390/atmos6050677](https://doi.org/10.3390/atmos6050677).
- PINIEWSKI, M., M. SZCZEŚNIAK, I. KARDEL, T. BEREZOWSKI, T. OKRUSZKO, R. SRINIVASAN, D.V. SCHULER, Z.W. KUNDZEWICZ in review: Hydrological modelling of the Vistula and Odra river basins using SWAT. – *Hydrol. Sci. J.*
- PIOTROWSKI, P., J. JĘDRUSZKIEWICZ, 2013: Projections of thermal conditions for Poland for winters 2021–2050 in relation to atmospheric circulation. – *Meteorol. Z.* **22**, 569–575. DOI: [10.1127/0941-2948/2013/0450](https://doi.org/10.1127/0941-2948/2013/0450).
- PLUNTKE, T., S. SCHWARZAK, K. KUHN, K. LUNICH, M. ADYNKIEWICZ-PIRAGAS, I. OTOP, B. MISZUK, 2016: Climate analysis as a basis for a sustainable water management at the Lusatian Neisse. – *Meteor. Hydrol. Water Manag. Res. Operat. Appl.* **4**, 3–11.
- PREIN, A., A. GOBIET, H. TRUHETZ, K. KEULER, K. GÖRGEN, C. TEICHMANN, C. FOX MAULE, E. VAN MEIJGAARD, M. DÉQUÉ, G. NIKULIN, R. VAUTARD, A. COLETTE, E. KJELLSTRÖM, D. JACOB, 2016: Precipitation in the EURO-CORDEX 0.11° and 0.44° simulations: High resolution, High benefits? – *Clim. Dyn.* **46**, 383–412. DOI: [10.1007/s00382-015-2589-y](https://doi.org/10.1007/s00382-015-2589-y).
- PROESTOS, Y., G.K. CHRISTOPHIDES, K. ERGÜLER, M. TANARHTE, J. WALDOCK, J. LELIEVELD, 2015: Present and future projections of habitat suitability of the Asian tiger mosquito, a vector of viral pathogens, from global climate simulation. – *Phil. Trans. R. Soc.* **B370**, 20130554. DOI: [10.1098/rstb.2013.0554](https://doi.org/10.1098/rstb.2013.0554).
- ROMANOWICZ, R.J., E. BOGDANOWICZ, S.E. DEBELE, J. DOROSZKIEWICZ, H. HISDAL, D. LAWRENCE, H.K. MERESA, J.J. NAPIÓRKOWSKI, M. OSUCH, W.G. STRUPCZEWSKI, D. WILSON, W.K. WONG, 2015: Climate Change Impact on Hydrological Extremes: Preliminary Results from the Polish-Norwegian Project. – *Acta Geophysica* **64**, 477–509. DOI: [10.1515/acgeo-2016-0009](https://doi.org/10.1515/acgeo-2016-0009).
- SEDLÁČEK, J., R. KNUTTI, 2014: Half of the world's population experience robust changes in the water cycle for a 2°C warmer world. – *Env. Res. Lett.* **9**, 044008. DOI: [10.1088/1748-9326/9/4/044008](https://doi.org/10.1088/1748-9326/9/4/044008).
- SORTEBERG, A, I. HADDELAND, J.E. HAUGEN, S. SBOŁOWSKI, W.K. WONG, 2014: Evaluation of distribution mapping based bias correction methods. – Norwegian Centre for Climate Services (NCCS) Report no. 1/2014, 23 pp.
- STANISŁAWSKA, K., Z.W. KUNDZEWICZ, K. KRAWIEC, 2013: Hindcasting global temperature by evolutionary computation. – *Acta Geophys.* **61**, 732–751. DOI: [10.2478/s11600-012-0091-z](https://doi.org/10.2478/s11600-012-0091-z).
- SZWED, M., G. KARG, I. PIŃSKWAR, M. RADZIEJEWSKI, D. GRACZYK, A. KĘDZIORA, Z.W. KUNDZEWICZ, 2010: Climate change and its effect on agriculture, water resources and human health sectors in Poland. – *Natural Hazards Earth Sys. Sci* **10**, 1725–1737. DOI: [10.5194/nhess-10-1725-2010](https://doi.org/10.5194/nhess-10-1725-2010).
- THEMESSL, M.J., A. GOBIET, A. LEUPRECHT, 2010: Empirical-statistical downscaling and error correction of daily precipitation from regional climate models. – *Int. J. Climatol.* **31**, 1530–1544, DOI: [10.1002/joc.2168](https://doi.org/10.1002/joc.2168).
- VAN DER LINDEN, P., J.F.B. MITCHELL, 2009: ENSEMBLES: Climate Change and its Impacts: Summary of research and results from the ENSEMBLES project. – Met Office Hadley Centre, FitzRoy Road, Exeter EX1 3PB, UK. 160 pp., http://ensembles-eu.metoffice.com/docs/Ensembles_final_report_Nov09.pdf.
- VAUTARD, R., A. GOBIET, S. SOBOLEWSKI, E. KJELLSTRÖM, A. STEGEHUIS, P. WATKISS, T. MENDLIK, O. LANDGREN, G. NIKULIN, C. TEICHMANN, D. JACOB, 2014: The European climate under a 2°C global warming. – *Env. Res. Lett.* **9**, 034006. DOI: [10.1088/1748-9326/9/3/034006](https://doi.org/10.1088/1748-9326/9/3/034006).

The pdf version (Adobe Java Script must be enabled) of this paper includes an electronic supplement:

Table of content – Supplementary Material

Figures S1, S2, S3, S4